Actinides

DOI: 10.1002/anie.200906127

# Neptunium Diverges Sharply from Uranium and Plutonium in Crystalline Borate Matrixes: Insights into the Complex Behavior of the Early Actinides Relevant to Nuclear Waste Storage**

*Shuao Wang, Evgeny V. Alekseev, Jie Ling, S. Skanthakumar, L. Soderholm, Wulf Depmeier, and Thomas E. Albrecht-Schmitt**

The immobilization of actinides, such as neptunium and plutonium, in solid matrixes is being used as an approach for preventing their release into the environment during long-term storage. Many waste forms have been suggested as being suitable, including zircon, garnet, pyrochlore, synroc, and monazite,[1] and there is an ongoing debate concerning the best waste form for actinides.[2–4] Among the earliest and most widely utilized solids for the storage and transport of actinides are borosilicate glasses.[5,6]

It has been recognized that both processing techniques and high actinide content in the glasses can lead to the formation of crystalline products within these glasses.[6] These crystals possess long-range order, are generally less soluble than the glasses, and display physicochemical properties that sharply contrast with the original glasses. Despite the importance of understanding the chemical nature of these crystals, very little is known about crystalline transuranium borates. In fact, there is not a single example present in crystallographic databases. In an effort to begin the process of understanding structure–property relationships in uranium, neptunium, and plutonium borates relevant to the development of advanced waste forms for the long-term storage of these radionuclides, we have prepared a large family of $U^{VI}$ borates, several highly unusual intermediate- or mixed-valent neptunium compounds, and a $Pu^{VI}$ borate that differs in bonding from its $U^{VI}$ counterparts.

Actinide borates are difficult to prepare by traditional methods, because water competes very successfully with borate for inner-sphere coordination sites for these metals under most conditions. In fact, many borates that occur naturally are found in evaporated deposits in arid regions.[7] This synthetic challenge can be overcome by either removing water entirely from the system in high-temperature solid-state reactions[8–13] or slow evaporations,[14] or by reducing the dielectric constant of water using hydrothermal conditions. We were initially interested in studying high-valence actinides, either $An^{VI}$ or $An^{V}$ (An = U, Np, Pu) and therefore avoided the potentially thermally reducing conditions of high-temperature solid-state reactions, and we diminished the potential for radiolytic reduction of the neptunium or plutonium in slow evaporation crystallizations that can take months to occur. Instead, we utilized a boric acid flux as the reaction medium by adding excess boric acid and various alkali-metal or alkaline-earth-metal nitrates to small droplets (ca. 5–20 μL) of 1.8 M $Np^{V}$, $Np^{VI}$, or $Pu^{VI}$ chloride or nitrate. Much larger scale (ca. 1 g) reactions were performed with uranium using a similar methodology. After three days of heating at approximately 220 °C in an autoclave and subsequent cooling, a single translucent crystalline mass was isolated. Within this mass, crystals were observed for all actinides studied. These crystals were freed from the matrix by the addition of hot water, which dissolved the excess boric acid flux, but even repeated washing leaves the crystals unaltered. Single-crystal and powder X-ray diffraction and spectroscopic measurements of these crystals then ensued.

The uranyl borates prepared to date number in excess of twenty. We have selected one of these for this discussion, $Na(UO_2)[B_6O_{10}(OH)]\cdot 2H_2O$.[15] Despite the complexity of this large family, there is a single fundamental building unit that exists for all of these compounds: a linear uranyl ($UO_2^{2+}$) cation surrounded by nine borate anions. This topology is substantially different from the topology observed when other triangular anions (e.g. carbonate) are combined with uranyl cations.[16] The borate anions, which occur as both $BO_3$ and $BO_4$ polymerized units, bridge between uranyl cations to create layers (Figure 1a). Additional $BO_3$ units extend perpendicular to these layers and link the layers together

[*] S. Wang, Dr. E. V. Alekseev, Dr. J. Ling, Prof. Dr. T. E. Albrecht-Schmitt
Department of Civil Engineering and Geological Sciences
and
Department of Chemistry and Biochemistry
University of Notre Dame, Notre Dame, IN 46556 (USA)
Fax: (+1) 574-631-9236
E-mail: talbrec1@nd.edu
Dr. E. V. Alekseev, Prof. Dr. W. Depmeier
Department of Crystallography, University of Kiel
24118 Kiel (Germany)
Dr. S. Skanthakumar, Dr. L. Soderholm
Chemistry Division, Argonne National Laboratory
Argonne, IL 60439 (USA)

[**] We are grateful for support provided by the Chemical Sciences, Geosciences, and Biosciences Division, Office of Basic Energy Sciences, Office of Science, Heavy Elements Program, U.S. Department of Energy, under Grants DE-FG02-01ER15187, DE-FG02-01ER16026. This material is based upon work supported as part of the Materials Science of Actinides, an Energy Frontier Research Center funded by the U.S. Department of Energy, Office of Science, Office of Basic Energy Sciences under Award Number DE-SC0001089, by Deutsche Forschungsgemeinschaft for support within the DE 412/30-2 research project, and under contract DE-AC02-06CH11357 at Argonne National Laboratory. We thank Professors Gregory S. Girolami and Peter C. Burns for helpful discussions.

Supporting information for this article is available on the WWW under http://dx.doi.org/10.1002/anie.200906127.

  

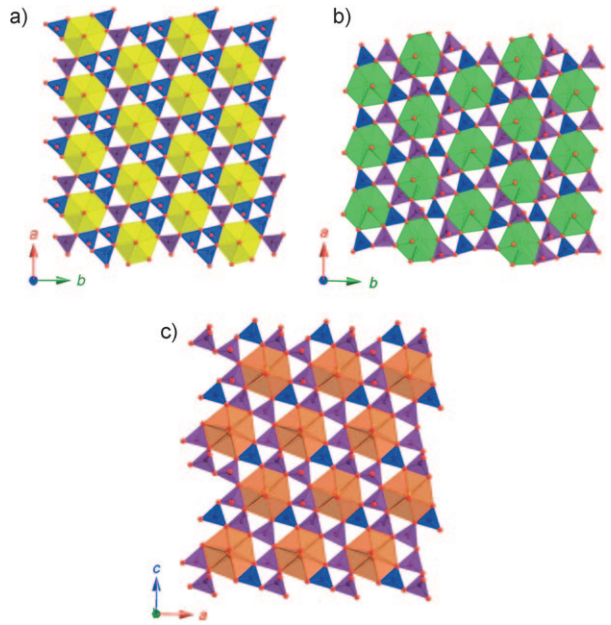


***Figure 1.*** Views of the a) uranyl, b) neptunyl, and c) plutonyl layers found in $Na(UO_2)[B_6O_{10}(OH)]\cdot 2H_2O$, $K_4(NpO_2)_{6.73}[B_{20}O_{36}(OH)_2]$, and $PuO_2[B_8O_{11}(OH)_4]$ showing the hexagonal bipyramidal environments around the $An^{VI}$ (An = U yellow, Np green, Pu orange) as well as the $BO_3$ triangles (blue) and $BO_4$ tetrahedra (purple).

into a polar three-dimensional framework with relatively large channels to house the $Na^+$ cations and the water molecules (Figure S1 in the Supporting Information). Despite the open-framework nature of this compound, it shows good thermal stability, loosing water at 180 °C and remaining intact until 500 °C.

The behavior of neptunium contrasts substantially with that of uranium. Two neptunium borates have been prepared that differ essentially only in their interlayer cations. The structures of $K_4(NpO_2)_{6.73}[B_{20}O_{36}(OH)_2]$ and $Ba_2(NpO_2)_{6.59}[B_{20}O_{36}(OH)_2]\cdot H_2O$ are extraordinary in all regards.[15] The overall structure is layered with slabs of neptunyl borate separated by $K^+$ or $Ba^{2+}$ cations. The layers diverge sharply from what is typically observed in high-valence actinyl oxoanion materials. They are approximately 1.6 nm thick. Most actinyl sheets have their thickness determined by a single polyhedron and are on the order of 4–5 Å. In this case, however, there are four distinct neptunium sites. In all cases the neptunium center is found in the form of an approximately linear dioxo cation, $NpO_2^{n+}$. An evaluation of both the neptunyl Np=O bond lengths and the bond-valence sums indicates that the four sites do not simply contain $Np^V$. In two of the sites the $NpO_2^{n+}$ cations are coordinated by six oxygen atoms in the equatorial plane to form $NpO_8$ hexagonal bipyramidal geometries. One $NpO_2^{n+}$ cation is bound by five oxygen atoms to form a $NpO_7$ pentagonal bipyramid. Bond-valence sum calculations suggest that the $NpO_8$ units are primarily +6 and the $NpO_7$ units primarily +5. The final $NpO_2^{n+}$ cation is bonded to four oxygen atoms to yield a tetragonal bipyramid. The core neptunyl unit has Np=O bonds that average 1.938(14) Å, which are considerable longer than those found in $Np^V$ compounds, which average 1.83(2) Å.[17] The neptunyl bond lengths and the bond-valence sum calculations indicate $Np^{IV}$.[17] However, it should be noted that a dioxo $Np^{IV}$ unit has never been observed before. The barium compound shows bond-valence sums more consistent with single oxidation states for each site, whereas there is slightly more intermediate valency in the potassium compound. Thus, in a single compound all possible coordination environments for neptunyl are realized, and there is evidence for three oxidation states for neptunium.

The neptunyl polyhedra are interconnected by both $BO_3$ and $BO_4$ units in the cases of the $NpO_7$ and $NpO_8$ units. However, the $NpO_6$ site is solely held in place by so-called cation–cation interactions (CCIs). These interactions form by the coordination of the "yl" oxo atoms from one neptunyl cation into the equatorial plane of a neighboring neptunium polyhedron. This Np site is flanked on two sides by $NpO_7$ units and on two sides by $NpO_8$ units that provide the CCI oxo atoms. The $NpO_6$ unit uses its oxo atoms to also form CCIs with the $NpO_7$ pentagonal bipyramids. While CCIs are known in approximately half of $Np^V$ oxoanion compounds,[17] this example is the first in which neptunium is solely held in place by CCIs. The bond-valence sum for this site of 4.0 valence units again suggests $Np^{IV}$ in the barium compound. The CCIs yield interconnected clusters of eleven neptunium centers within the layers (Figure 2 and Figure S2 in the Supporting Information).

The $BO_3$ and $BO_4$ units share corners to create highly complex sheets shown in Figure 2. Some of the oxygen atoms in these sheets are protonated to maintain charge balance for the structure. The joining of the $NpO_6$, $NpO_7$, $NpO_8$, $BO_3$, and $BO_4$ units creates the remarkable layers with nanoscale features. The layers are separated from one another by $K^+$ or $Ba^{2+}$ cations, some of which are ordered and some of which are disordered.

Bond-valence sum calculations, while effective in most cases, can only suggest possible oxidation states. The cavity size of the $NpO_6$ site might simply be too large, or there may

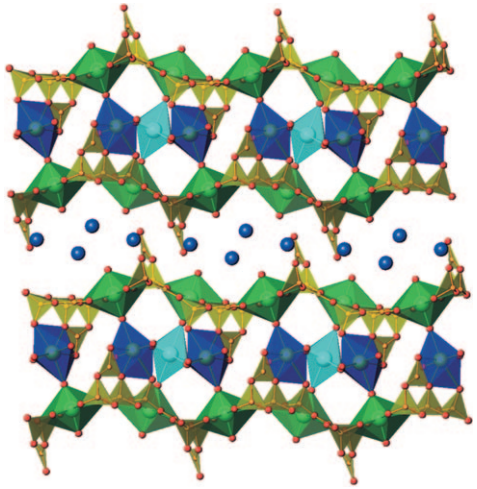

***Figure 2.*** Depiction of the structure of $K_4(NpO_2)_{6.73}[B_{20}O_{36}(OH)_2]$ or $Ba_2(NpO_2)_{6.59}[B_{20}O_{36}(OH)_2]\cdot 0.6H_2O$ showing $Np^{VI}O_8$ (green), $Np^VO_7$ (dark blue), and $Np^{IV}O_6$ (light blue) units linked by $BO_3$ triangles and $BO_4$ tetrahedra and by bridging oxo atoms to form 1.6 nm thick slabs that are separated by $K^+$ or $Ba^{2+}$ cations. Some of the disordered cations between the layers have been omitted for clarity.

  

be abnormalities associated with the partial occupancy, resulting in an anomalously low calculated charge. However, such considerations do not explain the lengthening of the neptunyl bonds. An excessively large cavity would probably result in a slight contraction of the neptunyl unit, not an expansion. The magnitude of the lengthening of the neptunyl bond is consistent with reduction of the oxidation state to a formal valence of +4. Nevertheless, much stronger evidence for $Np^{IV}$ comes from UV/Vis/NIR spectroscopic measurements taken from crystals of $K_4(NpO_2)_{6.73}[B_{20}O_{36}(OH)_2]$ and $Ba_2(NpO_2)_{6.59}[B_{20}O_{36}(OH)_2]\cdot H_2O$ using a microspectrophotometer. One convenient feature of the optical spectra of neptunium in different oxidation states is that they are very distinct from one another.[18,19] Absorption features are present that clearly identify $Np^{IV}$, $Np^{V}$, and $Np^{VI}$ Figure 3).[18,19] The most important f–f transitions for $Np^{IV}$ are the transitions near 700 and 800 nm, whereas the $Np^{V}$ and $Np^{VI}$ transitions are observed near 990 and 1200 nm, respectively. When calculations based on the known extinction coefficients of the f–f transitions and the measured intensities of the primary peaks for each oxidation state in the UV/Vis/NIR spectrum are compared with the crystal structures, the following formula based on formal oxidation states can be derived: $K_4(Np^{IV}O_2)_{0.73}(Np^{V}O_2)_2(Np^{VI}O_2)_4[B_{20}O_{36}(OH)_2]$ and $Ba_2(Np^{IV}O_2)_{0.59}(Np^{V}O_2)_2(Np^{VI}O_2)_4[B_{20}O_{36}(OH)_2]\cdot H_2O$. In short, the bond-valence sum calculations determined from the X-ray diffraction data are consistent with the spectroscopic measurements, and both indicate the first examples of a $Np^{IV}$ dioxo unit. Based on comparative studies using $Np^{VI}$ and $Np^{V}$ as the source of neptunium in these syntheses, it has been determined that this compound forms by the disproportionation of some of the $Np^{V}$ to yield $Np^{VI}$ and $Np^{IV}$. The fact that this compound forms with many different interlayer cations and from different oxidation states of neptunium suggests that it represents an energetic well.

Magnetization data for $K_4(NpO_2)_{6.73}[B_{20}O_{36}(OH)_2]$ as a function of temperature obtained under an applied field of 50 Gauss showed no evidence of any ordering down to the lowest measured temperature, 3.5 K. Field measurements at low temperature (5 K; 0–0.5 T) and higher temperature (300 K; 0–2 T) were linear, supporting the conclusion from the low-field, variable-temperature experiment. Zero-field cooled and field cooled data obtained as a function of temperature overlapped at all temperatures. Taken together, these results show the sample to be paramagnetic down to the lowest temperature measured. Susceptibility data used to obtain an effective moment (Figure S3 in the Supporting Information) were obtained at 0.5 T. Fitting these susceptibility data assuming Curie–Weiss behavior of non-interacting, localized moments produces an effective moment of (3.08 ± 0.15) $\mu_B$ per Np ion. The theoretical, free-ion effective moments, based on Russell Saunders coupling, are 3.62, 3.58, and 2.54 $\mu_B$ for $Np^{IV}$, $Np^{V}$, and $Np^{VI}$, respectively. These values represent maximum observables, because the crystal field is expected to reduce the measured moment. The measured moment represents an average over all the crystallographically distinct Np centers, weighted by their multiplicity, and as such cannot be analyzed in depth without extensive further experiments. However, it is interesting to note that if the susceptibilities are calculated assuming the free-ion moments weighted by the ratios of crystallographic multiplicities, a calculated effective moment of 3.01 $\mu_B$ per Np ion is obtained, well within the error of the experiment. The presence of neptunyl(V) and/or (IV) is confirmed by these results, because these valence states are required to increase the measured value above the theoretical value of 2.54 $\mu_B$ for $Np^{VI}$.

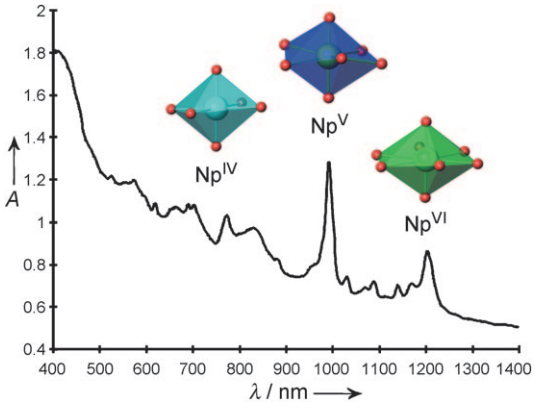


***Figure 3.*** UV/Vis/NIR spectrum of $K_4(NpO_2)_{6.73}[B_{20}O_{36}(OH)_2]$ showing regions of f–f transitions that indicate the presence of $Np^{IV}$, $Np^{V}$, and $Np^{VI}$. Corresponding $Np^{VI}O_8$, $Np^{V}O_7$, and $Np^{IV}O_6$ polyhedra are placed above each region of the spectrum.

Dichroic peach/pink crystals of $PuO_2[B_8O_{11}(OH)_4]$ were isolated as the sole product of the boric acid flux reactions with plutonium.[15] UV/Vis/NIR studies clearly show only $Pu^{VI}$ in the compounds (i.e. no reduction has taken place; Figure S4 in the Supporting Information).[18] At first glance the structure of this compound appears similar to that of many of the uranyl borates, because it also contains a hexagonal bipyramidal environment around the $Pu^{VI}$ centers. However, while there are still nine borate groups around the equatorial plane of the plutonium center, the number of $BO_3$ and $BO_4$ groups differs between $U^{VI}$ and $Pu^{VI}$ (see Figure 1c). In $PuO_2[B_8O_{11}(OH)_4]$ there are seven $BO_4$ units and two $BO_3$ units, whereas in $Na(UO_2)[B_6O_{10}(OH)]\cdot 2H_2O$ there are six $BO_4$ units and three $BO_3$ units. In the neptunium compounds the layers are also subtly different, as shown in Figure 1b. One way of viewing these layers is to consider them as being composed of chains of $BO_4$ tetrahedra that are linked into sheets by $BO_3$ triangles. There are further differences in the interlayer borate units; in all uranyl compounds there are only $BO_3$ triangles connecting layers, whereas in $PuO_2[B_8O_{11}(OH)_4]$ there are $BO_4$ tetrahedra between the layers, as shown in Figure 4. The three-dimensional network found for this material is also polar, as indicted by the monoclinic space group *Cc*. The origin of the acentricity is likely the helical nature of chains of $BO_3$ triangles (see Figure S1 in the Supporting Information), whose twisting reduces the interlayer space in these materials.

In conclusion, these data point to the mounting body of evidence that indicates the need to conduct research on the actual actinide in question and not on a less radioactive surrogate such as uranium.[20–23] However, this is not the primary message of this work. What we have now observed in $K_4(NpO_2)_{6.73}[B_{20}O_{36}(OH)_2]$ and $Ba_2(NpO_2)_{6.59}$-

  

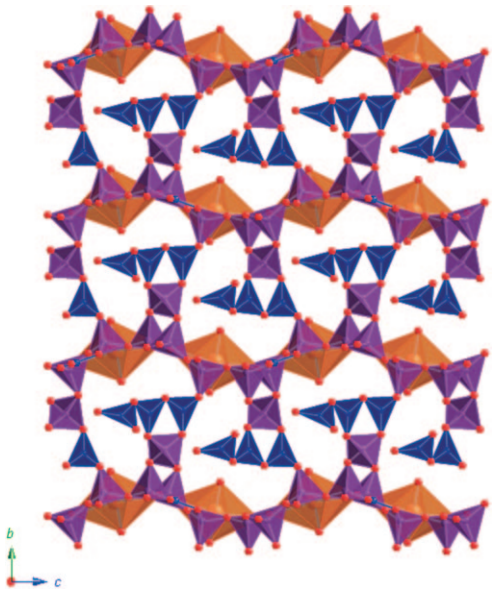


***Figure 4.*** A depiction of the polar, three-dimensional network found for $PuO_2[B_8O_{11}(OH)_4]$. $PuO_8$ hexagonal bipyramids are shown in orange, $BO_3$ triangles in blue, and $BO_4$ tetrahedra in purple. Unlike the uranyl and neptunyl borate phases, there are $BO_4$ tetrahedra between the layers.

$[B_{20}O_{36}(OH)_2]\cdot H_2O$ are materials that can successfully sequester all stable oxidation states of neptunium, not just one. Therefore, we have the ability to design advanced materials that target not just one oxidation state of a radionuclide but all possible oxidation states. The low-symmetry, polymeric nature of the borate anions is the key to achieving this goal, and therefore other polyanions (e.g. silicates and borophosphates) may also be appropriate for materials design. The neptunium borates underscore the need for more versatile storage materials most strongly, because unlike other actinides, neptunium's most stable oxidation state under normal environmental conditions is +5, in the form of $NpO_2^+$. This cation is notorious for being only weakly bound by anions and mineral surfaces and easily migrating in the environment. Neptunium is of particular importance because $^{237}Np$ has a long half-life ($t_{1/2} = 2.14\times10^6$ years), and in the long term will be the primary contributor to the calculated dose from spent nuclear fuel stored in repositories.[24]

## Experimental Section

Stock solutions of $^{237}Np^{VI}$ nitrate or $^{242}Pu^{VI}$ nitrate (0.037 M) were prepare by first digesting $NpO_2$ or $PuO_2$ in 8 M $HNO_3$ for 3 days at 200 °C (in an autoclave). The solutions were reduced to moist residues and redissolved in water. For plutonium, the solution was then ozonated for approximately 5 h to ensure complete oxidation of the plutonium to +6. UV/Vis/NIR spectroscopy indicates that only $Pu^{VI}$ is present. $Np^V$ stock solutions were prepared by reduction with nitrite and subsequent precipitation with hydroxide, washing, and dissolution in dilute HCl. Standard precautions were performed for handling radioactive materials during work with uranium. *$^{237}Np$ ($t_{1/2} = 2.14\times10^6$ y) and $^{242}Pu$ ($t_{1/2} = 3.76\times10^5$ y) pose serious health risks owing to their α and γ emission.* All studies with neptunium and plutonium were conducted in a lab dedicated to studies on trans-uranium elements.

Received: October 30, 2009
Published online: January 18, 2010

**Keywords:** actinides · borates · mixed-valent compounds · redox chemistry · solid-state reactions

[1] S. Krivovichev, *Minerals as Advanced Materials I*, **2008**, Springer, Heidelberg.
[2] I. Farnan, H. Cho, W. J. Weber, *Nature* **2007**, *445*, 190–193.
[3] R. C. Ewing, *Nature* **2007**, *445*, 161–162.
[4] R. C. Ewing, *Proc. Natl. Acad. Sci. USA* **1999**, *96*, 3432–3439.
[5] W. G. Ramsey, Glass as a Waste Form and Vitrification Technology: Summary of an International Workshop, **1996**, National Academy of Science Washington.
[6] T. F. Meaker, Neptunium Immobilization and Recovery Using Phase Separated Glasses, **1996**, Department of Energy.
[7] P. C. Burns, J. D. Grice, F. C. Hawthorne, *Can. Mineral.* **1995**, *33*, 1131–1151.
[8] M. Gasperin, *Acta Crystallogr. Sect. C* **1987**, *43*, 1247–1250.
[9] M. Gasperin, *Acta Crystallogr. Sect. C* **1987**, *43*, 2031–2033.
[10] M. Gasperin, *Acta Crystallogr. Sect. C* **1987**, *43*, 2264–2266.
[11] M. Gasperin, *Acta Crystallogr. Sect. C* **1988**, *44*, 415–416.
[12] M. Gasperin, *Acta Crystallogr. Sect. C* **1989**, *45*, 981–983.
[13] M. Gasperin, *Acta Crystallogr. Sect. C* **1990**, *46*, 372–374.
[14] H. Behm, *Acta Crystallogr. Sect. C* **1985**, *41*, 642–645.
[15] Crystallographic data for $Na(UO_2)[B_6O_{10}(OH)]\cdot 2H_2O$: Yellow-green block, 0.162 × 0.154 × 0.126 mm, monoclinic, space group *Cc*, $Z = 4$, $a = 6.3905(9)$, $b = 11.1390(15)$, $c = 15.987(2)$ Å, $\beta = 92.777(2)°$, $V = 1136.7(3)$ Å$^3$ ($T = 293(2)$ K), $\mu = 144.08$ cm$^{-1}$, $R_1 = 0.0416$, $wR2 = 0.1042$. $K_4(NpO_2)_{6.73}[B_{20}O_{36}(OH)_2]$: Drab plate, 0.105 × 0.042 × 0.011 mm, triclinic, space group $P\bar{1}$, $Z = 1$, $a = 6.5341(15)$, $b = 10.908(2)$, $c = 16.042(4)$ Å, $\alpha = 95.946(3)$, $\beta = 96.240(3)$, $\gamma = 90.162(3)°$, $V = 1130.3(4)$ Å$^3$ ($T = 293(2)$ K), $\mu = 158.35$ cm$^{-1}$, $R_1 = 0.0607$, $wR2 = 0.1491$. $Ba_2(NpO_2)_{6.59}[B_{20}O_{36}(OH)_2]\cdot H_2O$: Drab plate, 0.088 × 0.063 × 0.009 mm, triclinic, space group $P\bar{1}$, $Z = 1$, $a = 6.5582(13)$, $b = 11.016(2)$, $c = 17.071(3)$ Å, $\alpha = 100.927(3)$, $\beta = 100.497(3)$, $\gamma = 90.178$ (3)°, $V = 1189.7(4)$ Å$^3$ ($T = 293(2)$ K), $\mu = 160.33$ cm$^{-1}$, $R_1 = 0.0490$, $wR2 = 0.0853$. $PuO_2[B_8O_{11}(OH)_4]$: Dichroic peach/pink plate, 0.110 × 0.081 × 0.008 mm, monoclinic, space group *Cc*, $Z = 4$, $a = 6.4391(8)$, $b = 16.714(2)$, $c = 10.9648(13)$ Å, $\beta = 90.744(1)°$, $V = 1180.0(3)$ Å$^3$ ($T = 100(2)$ K), $\mu = 56.97$ cm$^{-1}$, $R_1 = 0.0198$, $wR2 = 0.0438$. Further details on the crystal structure investigation may be obtained from the Fachinformationszentrum Karlsruhe, 76344 Eggenstein-Leopoldshafen, Germany (fax: (+49) 7247-808-666; e-mail: crysdata@fiz-karlsruhe.de), on quoting the depository numbers CSD-420984, 420985, 420986, and 420987.
[16] P. C. Burns, *Can. Mineral.* **2005**, *43*, 1839–1894.
[17] T. Z. Forbes, C. Wallace, P. C. Burns, *Can. Mineral.* **2008**, *46*, 1623–1645.
[18] L. R. Morss, N. M. Edelstein, J. Fuger, *The Chemistry of the Actinide and Transactinide Elements*, **2006**, Springer, Heidelberg.
[19] H. A. Friedman, L. M. Toth, *J. Inorg. Nucl. Chem.* **1980**, *42*, 1347–1349.
[20] A.-G. D. Nelson, T. H. Bray, T. E. Albrecht-Schmitt, *Angew. Chem.* **2008**, *120*, 6348–6350; *Angew. Chem. Int. Ed.* **2008**, *47*, 6252–6254.
[21] A. E. V. Gorden, D. K. Shuh, B. E. F. Tiedemann, R. E. Wilson, J. Xu, K. N. Raymond, *Chem. Eur. J.* **2005**, *11*, 2842–2848.
[22] N. Dacheux, N. Clavier, G. Wallez, M. Quarton, *Solid State Sci.* **2007**, *9*, 619–627.
[23] S. D. Reilly, M. P. Neu, *Inorg. Chem.* **2006**, *45*, 1839–1846.
[24] J. P. Kaszuba, W. H. Runde, *Environ. Sci. Technol.* **1999**, *33*, 4427–4433.

  